

# A Detection Method of Ice Accretion Based on Flash Pulse Infrared Thermography

LI Qingying<sup>1\*</sup>, GOU Yi<sup>1</sup>, LIU Senyun<sup>2</sup>, YAO Rao<sup>1</sup>

1. School of Air Transportation, Shanghai University of Engineering Science, Shanghai 201620, P.R. China;

2. Key Laboratory of Icing and Anti/De-icing, China Aerodynamics Research and Development Center, Mianyang 621000, P.R. China

(Received 9 March 2023; revised 31 July 2023; accepted 13 August 2023)

**Abstract:** Ice detection plays a crucial role in operation of anti/de-icing systems. An ice detection method exploiting infrared thermal wave detection technology was proposed, followed by the identification of the edge, thickness and shape reconstruction of ice accretion using the related processing techniques. An active infrared ice detection experimental platform was constructed by flash pulse infrared technology. With regular and step-shaped ice samples prepared, the infrared thermal signals of the ice accretion were captured by an infrared thermal imager. A comparative analysis of the edge detection effects was conducted between the traditional edge detection methods and a new edge detection algorithm combining Gaussian-Laplacian pyramids and area filtering. Through the spatiotemporal correlation of the ice thermal signal, an end-to-end infrared detection ice thickness prediction model (i.e., convolutional neural network-long short term memory-efficient channel attention (CNN-LSTM-ECA)) was constructed by introducing the attention mechanism into the LSTM model, with the thickness of the ice predicted. Further, three-dimensional reconstruction of ice accretion was performed by combining the edge detection and thickness prediction. It concluded that both traditional and new edge detection algorithms based on Gaussian-Laplacian pyramids and area filtering can be used to detect the outer edge of the ice, but the new algorithm shows a significant advantage in detecting the ice edge with internal step boundaries. The CNN-LSTM-ECA thickness prediction model based on signal features performs well in prediction accuracy, stability, and noise resistance. The data for reconstructing three-dimensional ice accretion shape come from the collected digital signals and thermal images, which are not limited by temperature reading and heat transfer conditions, and have a wider application prospect. This paper provides a reference for exploring an effective accurate and quantitative identification method for ice accretion detection based on flash pulse infrared thermography.

**Key words:** ice accretion; infrared detection; edge detection; thickness prediction; three-dimensional shape reconstruction

**CLC number:** V248.1

**Document code:** A

**Article ID:** 1005-1120(2023)S1-0105-13

## 0 Introduction

Airplane icing refers to a circumstance where ice accumulates on the surface of certain parts of the airplane, which is one of the major safety risks posed to the flight. Airplane icing threatens the safety, maneuverability, and stability of the aircraft, which can lead to catastrophe in some circumstances<sup>[1]</sup>. Thus, it is essential to detect and prevent air-

plane icing effectively. Accurately identifying the geometric structure of ice accretion on the key surfaces of aircraft is one of the problems needing to be solved for the development of anti-icing technology.

Icing detection is the premise of anti/de-icing work. Usually, icing losses and hazards can be reduced by accurately detecting the severity of ice accretion on the protective surface, measuring the range and thickness of ice accretion, as well as trans-

\*Corresponding author, E-mail address: liqy\_2013@163.com.

**How to cite this article:** LI Qingying, GOU Yi, LIU Senyun, et al. A detection method of ice accretion based on flash pulse infrared thermography[J]. Transactions of Nanjing University of Aeronautics and Astronautics, 2023, 40(S1): 105-117.

<http://dx.doi.org/10.16356/j.1005-1120.2023.S1.010>

mitting the relevant information to the controller or alerting the workers to the need for countermeasures. Due to the insufficient demand for ice shape data measurement, the methods of ice shape measurement, such as manual tracking<sup>[2]</sup> and casting<sup>[3]</sup>, were widely used. However, the growing demand for accurate ice shape data has led to the emergence of more advanced techniques, e. g. non-contact ice shape measurement. Struck et al.<sup>[4]</sup> made use of multiple static cameras, high-speed cameras, and high-definition cameras to capture the image of ice on airplane wings from multiple angles. Then, the images were processed to extract the contour of ice accretion, with the thickness and growth rate of the ice measured. Through the non-contact measurement of the ice shape by optical camera, Ikidaes et al.<sup>[5]</sup> solved the problem that the ice shape was damaged during the measurement performed to obtain one-dimensional or two-dimensional ice shape data. However, the accuracy of measurement affected by the interference from clouds and fog. Gong et al.<sup>[6]</sup> performed laser sheet scanning to measure the time evolution of three-dimensional rime ice shape. In the icing wind tunnel, the growth of ice was effectively measured. Wang et al.<sup>[7]</sup> arranged conventional ice detectors at different sensitive icing locations according to the collection range of water droplets to detect the whole ice environment.

Given the advantages and disadvantages of various ice detection methods, along with the difficulty in quantifying the geometrical shape of ice with most icing sensors, it is difficult to collect more information than the thickness of ice and three-dimensional or even two-dimensional information. Therefore, there is an urgent need to develop an ice detection method that can be used to obtain the accurate information about ice shape. However, icing during flight is a dynamic and complex process, and ground maintenance personnel often observe the static ice accretion and carry out anti/de-icing operations with the detection results. Especially, maintenance personnel also conduct visual inspection, manually touching the certain surface of the aircraft to check for ice accumulation. Thus, a feasibility study on static ice accretion detection was discussed

using non-contact flash pulse infrared thermal detection technology according to experimental conditions, focusing on three aspects: Ice edge detection for icing range, ice thickness prediction, and ice shape reconstruction. Infrared detection technology is characterized by extensive applicability, no contact, fast detection, high accuracy, the minimal impact from cloud/fog/lighting, the ease of qualitative and quantitative analyses, and intuitive visualization. Therefore, it has been widely used in aerospace, automobile, military, new material research, the petrochemical industry, the nuclear industry, and the power industry<sup>[8]</sup>. Riehm et al.<sup>[9]</sup> proposed the use of an infrared thermometer to detect road icing, allowing the monitoring of temperature changes caused by the exothermic reaction of water freezing. Rashid et al.<sup>[10]</sup> used infrared thermal imaging technology to record the thermal response of sea ice, and determined the correlation between response time and ice layer thickness through calculation. Grzych et al.<sup>[11]</sup> used infrared satellites to capture the radiation of ice accretion, but at high cost. Gao et al.<sup>[12]</sup> adopted an infrared multispectral detection system to detect the residual ice on airplane wings during ground experiments.

Edge identification of ice accretion, i. e., ice range detection, plays an essential role in the detection of ice accretion, which is a prerequisite for triggering the anti/de-icing systems. The recognition of ice thickness is required to guide the energy output of the systems as well. Therefore, an infrared thermography system is used in this paper to explore how the edge and thickness of ice accretion can be identified and determined using different image processing methods. Further, by combining the edge detection and thickness of ice accretion, a three-dimensional ice shape can also be reconstructed to provide more accurate guidance for anti/de-icing operations.

## 1 Experiments and Materials

The rationale of the pulsed infrared thermography ice detection is to heat the ice adhered layer with a flashing lamp as the source of thermal excitation. As the ice surface emits thermal waves, it infiltrates the ice. During ice detection, a thermal cam-

era is used to record the changes in the thermal signal caused by the infiltration of the thermal waves into the ice. Then, the thermal imaging results are obtained to identify the morphology of ice accretion.

Based on the above rationale of ice infrared thermography detection, an infrared thermography testing platform was constructed in this paper. As shown in Fig.1(a), the infrared camera is an InSb infrared camera, consisting of an internal circulation Stirling cooler and a CdHg-Te (MCT) focal plane detector. This camera has a resolution of  $640 \text{ pixel} \times 512 \text{ pixel}$ , and a spectral range of  $2.0\text{--}5.7 \mu\text{m}$ . Also, the  $2 \times 2$  matrix of xenon flash lamps with a total power supply of 12 kJ is used for active thermal wave excitation, as illustrated in Fig.1(b). In this paper, we consider the examples of regular ice accretion because they are easier to be applied in practice. Multiple ice samples are prepared inside a refrigerated freezer in Fig.1(c), including the regular rectangular ice blocks and step-type ice blocks intended for edge and thickness identification, as shown in Fig.2. Immediately after the ice samples were prepared, they were placed under the infrared camera, with the energy output of the xenon lamps adjusted to record the changes in surface temperature of the ice under active excitation.

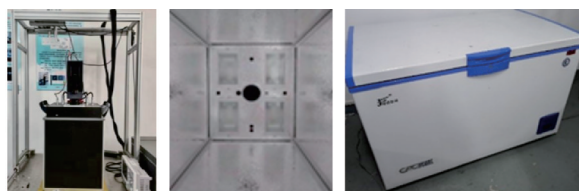


Fig.1 Infrared equipment for ice detection

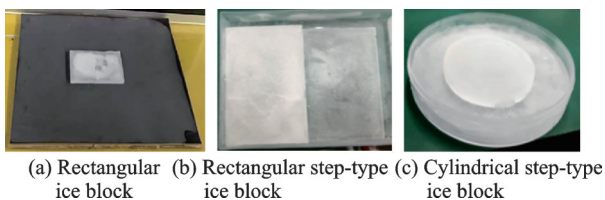


Fig.2 Physical samples of ice

## 2 Edge Detection of Ice Accretion

### 2.1 Edge detection method

#### 2.1.1 Traditional methods

Edge detection of ice accretion reflecting the ic-

ing range is considered a prerequisite for the detection of ice accretion. However, the results of infrared thermal wave detection are easily affected by the environmental conditions, thus leading to various problems such as the fusion of infrared images with the background and uneven illumination. This poses a challenge for detecting ice accretion through infrared thermal wave detection technology. Therefore, the first step in accurate ice detection is to use suitable algorithms to identify the boundary lines of ice through infrared thermal wave detection technology. Some research have dealt with ice detection image processing through traditional edge detection operators, fusion-improved edge detection operators, and a combination of threshold segmentation and morphology. In Ref.[13], the algorithm based on wavelet transform, floating threshold, digital image morphology, and optimal threshold fusion is used to identify the ice boundary line. In Ref. [14], the adaptive segmentation threshold method is used to determine the shape of ice accretion.

The purpose of edge detection is to find a set of pixels with a numerically abrupt change in the pixel values from the image, which are usually represented by edges in the image. At the same time, edge detection is performed to effectively suppress the non-main information in the image and preserve the important structural properties of the image. Given some differences in the ideas of different edge detection operators and variations in the structural properties of image features, it is currently difficult to obtain the same edge by using the same edge detection operator for the images with different structural properties<sup>[15]</sup>.

Among them, the traditional edge detection operators are built through first-order or second-order differential processing on the image, such as the Roberts operator, Sobel operator, and Prewitt operator, which are common first-order differential operators, as well as the Laplacian operator and Canny operator, which are common second-order differential operators<sup>[16]</sup>. The Roberts operator calculates the edges through local differences, the convolution template of a  $2 \times 2$  matrix both horizontally and vertically. However, the Roberts operator is highly sen-

sitive to noise and ineffective in suppressing noise. As an optimization of the Roberts operator, the Prewitt operator identifies the edges by performing the first-order differentiation of adjacent pixels in the image. That is to say, the gray values in the horizontal and vertical directions are not normalized for the mean difference. Therefore, the Prewitt operator is suitable for image smoothing, but the edge recognition is not accurate enough. The Sobel operator achieves an improvement on the Prewitt operator, with a  $3 \times 3$  matrix as its convolution template. The gray values of adjacent pixels in the horizontal and vertical directions are weighted and averaged, while the gray difference approximation value of the image is obtained through the convolution template. When the gray difference approximation value exceeds a certain threshold, it is judged as an edge. Therefore, the Sobel operator produces a smoothing effect on the image noise and can be used to determine the direction of the edge accurately. Differently, the Laplacian operator and Canny operator are classed into second-order differential operators. Among them, the Laplacian operator is a second-order differential operator in  $n$ -dimensional Euclidean space, defined as the divergence of the gradient. It is more accurate in locating the edge and sharpening the image. The Canny operator, as a more common edge detection operator, can be used to extract edges accurately while suppressing noise effectively. In addition, the phase coherence method is applicable to detect the edge in infrared images, and the edge can be identified by classifying the points with a high degree of phase coherence through K-means.

### 2.1.2 Improved method

When there is a lack of uniformity in the thickness of an ice accretion sample, the boundary in the infrared image of the sample is unclear and is more likely to be affected by the environment where detection is carried out. Therefore, traditional edge detection methods are not applicable to find the ideal surface boundary. Additionally, traditional infrared image threshold segmentation and edge detection techniques can be relied on only solving a specific type of problem for the processing of ice accretion sample infrared image<sup>[17]</sup>.

Aiming to address this situation, the traditional edge detection operator is improved in this paper to identify the surface boundary of ice accretion more accurately. To achieve the desired effect, the Gaussian-Laplacian pyramid operator is combined with area filtering to solve the problem that the internal boundaries are inaccurately detected due to the indistinct grayscale differences between step and non-step regions in the infrared image. On this basis, the ice surface boundary can be identified<sup>[18]</sup>. The Gaussian-Laplacian pyramid is comprised of a Gaussian filter function and a Laplacian operator<sup>[19]</sup>. The Gaussian pyramid is intended to decompose the image by gradually sampling it downwards, with the Gaussian filtering of the original image performed before sampling. The Gaussian filter formula and Gaussian pyramid formula are shown as follows

$$g(x, y) = \frac{1}{2\pi\delta^2} e^{-\frac{x^2+y^2}{2\pi\delta^2}} \quad (1)$$

$F(n+1) = F(n) \times g(x, y) \times S(\text{scale } 1, \text{scale } 2)$  (2) where  $F(n)$  represents the  $n$ th decomposition of the image and  $S(\text{scale } 1, \text{scale } 2)$  the sampling rate of the image on the row and the column. In this case, the sampling rate for both rows and columns is 2. Thus, the size of each image after sampling is reduced to 1/4 that of the original image, and the resolution is reduced to 1/2 that of the original image<sup>[20]</sup>.

The purpose of the Laplacian pyramid is to preserve the residual difference between adjacent levels during the downward sampling by the Gaussian pyramid, i.e., the high-frequency details of the image. The Laplacian pyramid formula is shown as follows

$$L(n) = F(n) - F(n+1) \times g(x, y) \times S(\text{scale } 1, \text{scale } 2) \quad (3)$$

The detailed process is shown in Fig.3. Firstly, the Gaussian-Laplacian pyramid operator is used to highlight the high-frequency structure of the image, which enhances the feature information of the image. Secondly, the small noise is filtered out by area filtering to preserve the edge information of the image. The noise in the image and the image edges to be extracted can be treated as the connected regions with different area values in the binary image. On

this basis, the connected domain area of the Gaussian-Laplacian filtered image is calculated, and the connected domain with a relatively small area is inverted. Thirdly, the transformation of image morphology is performed to fuse the filtered image with the source image, thus deepening the structural information of the external and step-type internal boundaries. Finally, the Canny operator is used to perform edge detection on the grayscale image with enhanced feature information for identifying the ice accretion sample detection with step-type boundaries.

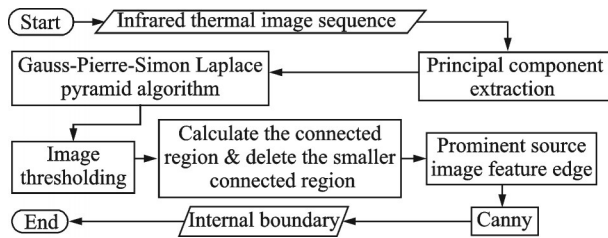


Fig.3 Flowchart of the edge detection algorithm

### 2.2 Results and discussion of edge detection

By performing traditional edge detection and using improved Gaussian-Laplacian pyramid and area filtering algorithms (Figs.4,5), the boundary de-

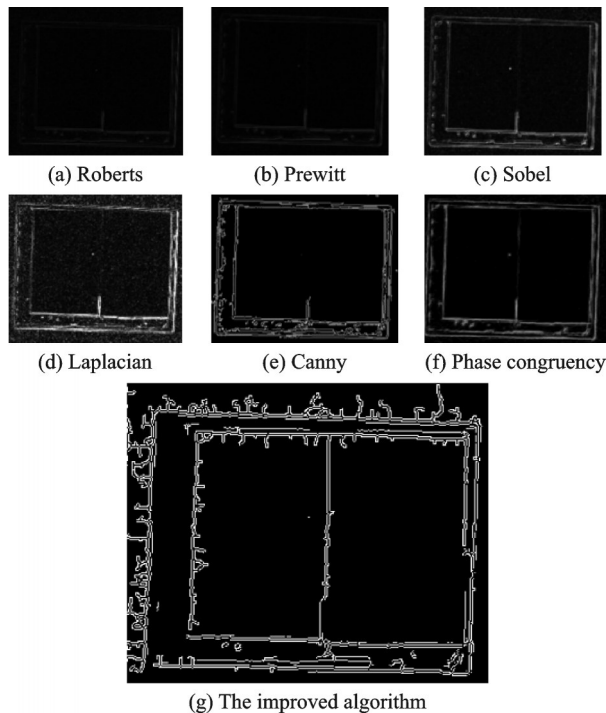


Fig.4 Results of traditional edge detection operators of stepped ice specimens on rectangular bodies

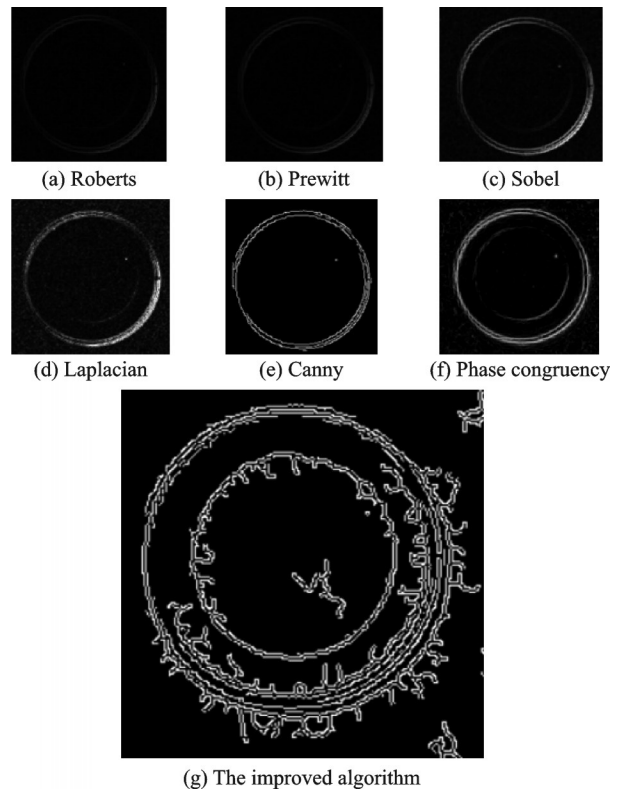


Fig.5 Results of traditional edge detection operators of stepped ice specimens on cylindrical bodies

tection results of infrared thermography of ice specimens were comparatively analyzed to reveal the following issues.

Traditional edge detection operators mainly extract the image edges by detecting the abrupt changes in the grayscale values of the image. Before the edge area is calculated, the traditional edge detection algorithm is first used to perform denoising and smoothing filtering on the image. Therefore, when the flash infrared detection is used to identify the surface boundary of regular and stepped ice samples, there is a significant abrupt change in the grayscale value of the external boundary of the regular ice sample. At this time, traditional edge detection algorithms can be used to detect the external boundary. However, traditional edge detection algorithms may fail to detect the internal stepped boundary of ice samples due to the non-identifiable changes to grayscale value in the infrared image of the stepped ice sample. Additionally, although the phase consistency algorithm is able to identify internal boundaries, it is not suitable to draw the high-phase-consistency edge area accurately and clearly due to the in-

significant phase consistency difference in the image.

The algorithm, which combines Gaussian-Laplacian pyramid and the area filtering proposed in this paper, is first used to extract the primary image components and structural information of the infrared ice detection sequence image. Then, the area filtering algorithm is used to filter out the noise unneeded for target detection, considering that the area of the connected region of noise in the grayscale image is smaller compared with the connected region of the internal and external edges of the image. Therefore, the algorithm combining Gaussian-Laplacian pyramid and area filtering can be applied to retain the image feature structure completely. Unlike traditional edge detection algorithms and phase congruency, it does not treat internal edges as noise, thus avoiding the failure to identify stepped internal edges.

The edge detection algorithm integrating Gaussian-Laplacian pyramid and area filtering gives priority to image features for denoising to be performed according to the overall image features. Thus, it does not treat the detection results as noise, which avoids the failure to recognize internal boundaries. However, the noise level in the detection results is higher than that of traditional algorithms. Therefore, the edge detection algorithm combining Gaussian-Laplacian pyramid and area filtering is advantageous in identifying irregular ice surfaces. Meanwhile, the drawback is that the noise in the image is highlighted when the high-frequency features of the image are preserved by the Gaussian-Laplacian operator due to much noise remaining in the infrared thermal sequence image. In addition, the shapes of the original ice accretion in this paper are regular. For other ice accretion shapes, edge detection methods are still applicable. Indeed, the relevant quantity for the ice shape detection method is the intensity profile of the pixels. As long as the intensity profile of the pixels describes the characteristics of the ice accumulation area, the collection of these pixels may be used to represent the ice accretion, regardless of the shape of the ice accumulation. In turn, the shape of ice accretion only affects the arrangement of the target pixels.

### 3 Thickness Prediction of Ice Accretion

#### 3.1 Thickness prediction methods

##### 3.1.1 Ice thickness prediction model

The thickness of ice accretion is an important indicator for the implementation of anti/de-icing systems. Although infrared thermography detection shows its advantage in detecting flat surfaces due to its temperature distribution characteristics, infrared detection mainly relies on the thermal state of the surface of testing objects and cannot visually determine the internal thermal state of the objects, thereby increasing the difficulty of thickness measurement. Thus, depth detection has become a research hotspot among scholars<sup>[21]</sup>. In the experiment on detecting ice thickness through infrared thermography, the transient heat varies with the thickness of the ice sample over time, and the signal of infrared thermography detection can be decomposed into spatial and temporal dimensions. When ice thickness is detected through infrared thermography, it can be viewed as a regression problem. The key to predicting ice thickness is to solve this problem<sup>[22]</sup>.

The traditional regression methods used to predict ice thickness through infrared detection ignore spatiotemporal correlation<sup>[23-24]</sup>, while a single convolutional neural network ignores the temporal features of the infrared detection signal. The long short-term memory (LSTM) model with fully connected layers gives no consideration to spatial correlation. To better simulate spatiotemporal relationships<sup>[25]</sup>, this paper proposes that the LSTM model can be extended to a convolutional model with convolutional results for the establishment of an end-to-end infrared detection ice thickness prediction model (i. e., convolutional neural network-long short-term memory-efficient channel attention (CNN-LSTM-ECA)) by introducing attention mechanism into the LSTM model<sup>[26-27]</sup>. Through this model, the errors in predicting ice thickness using infrared detection can be reduced for the improvement of accuracy.

Prediction of ice thickness through infrared detection requires time series analysis, which is also

affected by the physical spatial features. Traditional regression prediction models are capable only of extracting features from the infrared signal values when ice thickness is predicted, which leads to the lack of a description of complex spatiotemporal relationships and makes it difficult to estimate the impact of spatial and temporal information on the prediction results simultaneously. To address this issue, an end-to-end infrared detection ice thickness prediction model is proposed in this paper that combines LSTM with CNN and introduces the ECA attention mechanism.

The structure of the CNN-LSTM-ECA model is illustrated in Fig.6, where  $bs$  represents the batch size. The infrared detection signal of the ice sample is taken as the input data of the CNN-LSTM-ECA model. First of all, the model is used to extract the spatial dimension features of the signal through one-dimensional convolution. Then, it is used to extract the temporal features of the signal by introducing a gate-controlled recurrent unit with the attention mechanism. Finally, it relies on the fully connected layers to obtain the prediction result<sup>[28]</sup>.

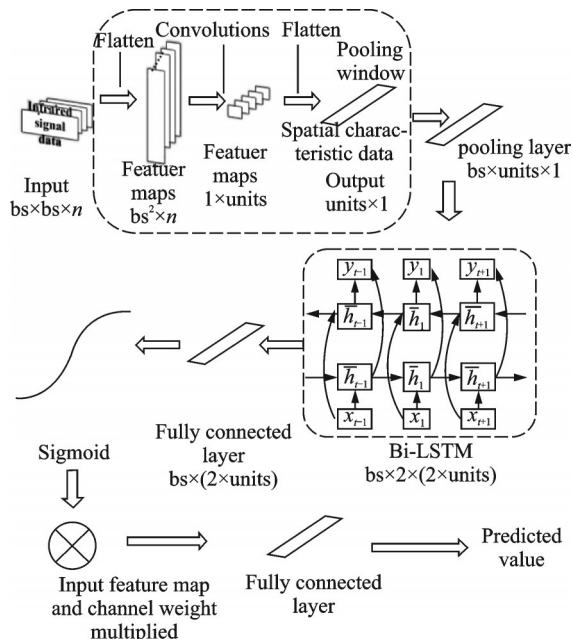


Fig.6 CNN-LSTM-ECA model structure diagram

### 3.1.2 Spatial feature extraction based on CNN

In the present study, a convolutional neural network (CNN) is employed to extract spatial features. According to the theory of thermal waves, the heat conducted by natural objects is usually

transferred along the  $x$ ,  $y$ , and  $z$  directions, and the distribution of temperature  $T$  is related to the space. The temperature field on the ice surface is affected by its neighboring spatial variables, and CNN is applicable to obtain the spatial features of data through the convolutional layers<sup>[29]</sup>.

Based on the assumption that the number of frames of infrared detection is identical to that of channels in the image, the signal value of each frame is taken as the grayscale value of the image, and the coordinate of each position on the ice sample is treated as the pixel coordinate of the image. Therefore, the experimental data can be considered as an image structure with  $n$  channels. Unlike traditional image definitions, the data in the current experiment show a pseudo-image structure with pixel values as digital signal values. To better express the spatial relationship, the space is denoted as  $G_{i,j}$ , while  $i$  and  $j$  represent the pixel coordinates corresponding to this space. To extract the target region  $G_{i,j}$ , the  $n$  channel numbers corresponding to all pixels in  $G$  are taken as the input.

Assuming that  $G$  contains  $bs^2$  pixels, the input data have a dimensional size of  $bs \times bs \times n$ , and that of  $G_{i,j}$  is  $1 \times 1 \times n$ . The input data are flattened into  $bs^2 \times n$  for convolution. Thus, the output of the convolutional neural network is obtained as follows

$$y = F(w^k G_{i,j} + b_v) \quad (4)$$

where  $y$  represents the spatial feature extracted from the current pixel point;  $w^k$  the convolution kernel; and  $b_v$  the bias term of the convolution kernel. The Sigmoid function is treated as the activation function. Finally, the spatial features are unfolded into one-dimensional sequential data for subsequent model operations. The structure of the convolutional model is illustrated in Fig.7.

### 3.1.3 Time feature extraction based on LSTM-ECA

When the detection of infrared ice accretion is carried out, the distribution of the surface temperature field  $T$  of ice accretion is affected by the time domain  $t$ . When the thickness of ice accretion varies, there are changes shown by the trend of the

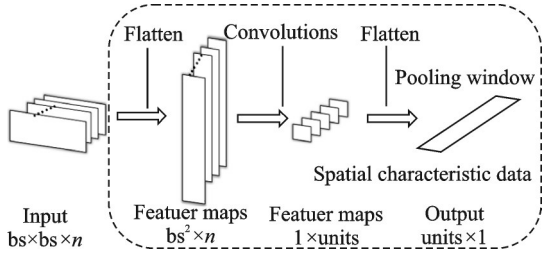


Fig.7 Structural diagram of the convolution model

temperature field on the ice surface over time. To address this issue, it is proposed in this paper to extract time features using the LSTM-ECA model block after the extraction of spatial features. Based on the ECA attention mechanism, the model can be used as shown in Fig.6.

The procedures of using the LSTM-ECA model are as follows:

**Step 1** The max pooling of data with spatial features extracted by the convolutional neural network is performed to reduce the number of hidden layer parameters, remove redundant information, and compress the features. This is also the first step of the ECA attention mechanism, through which the data  $x$  is obtained.

**Step 2** The dropout operation of data  $x$  is conducted to obtain  $x_1$ , which prevents the overfitting caused by the use of too many parameters given a small number of training samples.

**Step 3** Bi-LSTM operation is performed on the result  $x_1$  obtained in Step 2 to extract the time features of the data, resulting in  $x_2$ .

**Step 4** To address the nonlinearity of the data,  $x_2$  is inputted into the activation function Tanh, which is expressed as

$$\text{Tanh}(x) = \frac{\sinh(x)}{\cosh(x)} = \frac{e^x - e^{-x}}{e^x + e^{-x}} \quad (5)$$

This yields  $x_3$ .

**Step 5** The output of the fully connected layer replaces the convolutional layer output of the traditional ECA attention mechanism for a better integration with the Bi-LSTM network built in Step 3, which ensures the data dimension of the model, with the output data  $x_4$  obtained.

**Step 6** The Sigmoid activation function is used to calculate the weight  $w$  of  $x_4$ . ECA is essential for the attention mechanism, through which the

weight of each channel is determined.

**Step 7** The feature data  $x_4$  and channel weight  $w$  are multiplied to assign a greater weight for those important features, focus attention on important features, and obtain data  $x_5$ .

**Step 8** The fully connected operation of  $x_5$  is conducted to obtain the output data size of 1, which is the data size needing to be predicted by the model.

**Step 9** The activation function Tanh is used to calculate the predicted data as obtained in Step 8, with the final data as the predicted value.

In essence, the focus of ECA attention mechanism introduced into this model is on the information that is more critical to the current task than a large amount of other input information. It is used to reduce the sensitivity to other information and filter out the irrelevant information, which is conducive to improving the accuracy of time feature extraction and prediction.

### 3.2 Results and discussion of thickness prediction

By using random sampling method, the infrared detection signal of ice accumulation is randomly sampled, with each sample value labeled with the thickness of the ice sample corresponding to the sample point. For the convenience of expression, let  $S = \{s_1, s_2, \dots, s_i, \dots, s_n\}$  represent the sample point set, where  $s_i$  denotes the  $i$ th sample point, with each piece of sample data in  $s$  including 200 frames of infrared digital signals. The data are standardized to ensure the convergence of neural network training, with 70% of the above data taken as the training set and 30% as the test set to input the model for training and prediction.

The samples with an ice thickness of 1 cm or 3 cm are selected to conduct the experiment, in which the performance of 1D CNN is compared with that of LSTM, LSTM-CNN, and the proposed model. The prediction results are evaluated using mean squared error (MSE) and coefficient of determination ( $R^2\_score$ ). MSE and  $R^2\_score$  are expressed as Eqs.(6, 7), respectively.

$$\text{MSE} = \frac{1}{N} \sum_{t=1}^N (X_{\text{pred},t} - X_{\text{real},t})^2 \quad (6)$$



$$R^2 = 1 - \frac{\sqrt{\text{MSE}}}{N} \quad (7)$$

where  $N$  represents the number of sample points,  $X_{\text{pred},t}$  the predicted value of the  $t$ th sample point, and  $X_{\text{pred},t}$  the true value of the  $t$ th sample point.

As shown in Fig.8, the MSE of the model is gradually reduced with an increase in iterations during the training process. Among them, the single LSTM model has the largest initial loss value. The CNN-LSTM model performs poorly in convergence, while the single CNN model performs well. Compared with other models, the proposed CNN-LSTM-ECA model has a less significant prediction error and performs better in convergence.

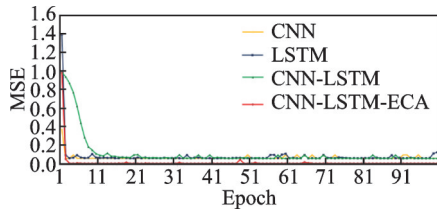


Fig.8 Training accuracy of CNN-LSTM-ECA model

After training of the model, ten test data points are randomly sampled as sample points, including five sample points with a 1 cm thickness and five sample points with a 3 cm thickness. Then, the prediction results obtained by different models are analyzed. Table 1 shows the prediction results of the samples with an ice thickness of 1 cm or 3 cm (rounded to two decimal places), and Table 2 lists the prediction errors of different network models. According to Tables 1, 2, the CNN-LSTM-ECA model has the least significant prediction error and

Table 1 Result of network model

Prediction value/cm	Actual value/cm			
	CNN	LSTM	CNN-LSTM	CNN-LSTM-ECA
3	2.56	2.98	2.96	2.98
3	2.96	2.98	2.97	2.97
3	2.96	2.97	2.97	2.97
3	2.97	2.98	2.98	2.97
3	2.97	2.98	2.98	2.97
1	0.99	1.05	1.02	1.01
1	1.02	1.05	1.00	1.00
1	1.00	1.05	0.99	1.00
1	0.99	1.05	0.99	1.00
1	0.99	1.05	0.99	1.00

the highest fitting degree, indicating its advantages in predicting the thickness of ice accretion based on infrared detection. This confirms the CNN-LSTM-ECA model can be used to extract time and space features from the infrared images of ice accretion. When using the CNN-LSTM neural network for training and testing, attention can be better focused on those important features through the introduction of the ECA mechanism, thereby improving the accuracy in predicting the thickness of ice accretion. Accordingly, the thickness prediction method is still effective for other shapes of ice accretion. The thickness of ice accretion was predicted by inputting the infrared signals corresponding to the pixels in the ice detection image into the proposed network model. Therefore, as long as the position of pixels in the ice detection image is determined, the thickness of ice accretion can be predicted without being affected by the ice shape. This method can be also used for three-dimensional reconstruction, and is independent of the specific ice shape.

Table 2 Comparison of network model predictions

Model	$R^2$ -score	MSE
CNN	0.91	0.06
LSTM	0.95	0.05
CNN-LSTM	0.91	0.05
CNN-LSTM-ECA	0.99	0.01

## 4 Three-Dimensional Reconstruction of Ice Accretion

### 4.1 Reconstruction methods

The three-dimensional reconstruction of infrared thermal images is a research focus of infrared detection technology, and can also be referenced in the detection of ice accretion. When detecting the presence of ice accretion, it is sometimes further required to identify the three-dimensional shape of ice accretion for more accurate guidance on the energy output of anti/de-icing systems, in addition to obtaining the covered range or thickness of ice accretion. In the existing three-dimensional reconstruction technology, the acquisition of three-dimensional data is mainly point cloud data through sensors such as depth sensors or laser radar to achieve effec-

tive reconstruction of three-dimensional models<sup>[30-31]</sup>. In this paper, edge detection and thickness prediction were combined to reconstruct the three-dimensional shape of ice accretion, as shown in Fig.9. The edge was detected by the detection algorithm combining Gaussian-Laplacian pyramids and area filtering in Section 2 to guide the range of ice thickness prediction. The surface morphology of the ice accretion was extracted based on the calculated contour of the ice sample. The data were refined while maintaining the original information to the greatest extent. The boundary contour of ice was drawn by setting thresholds and traversing all pixel gray values within the ice sample. The CNN-LSTM-ECA model in Section 3 was developed to predict the ice thickness within the ice accretion boundary range. The predicted one-dimensional thickness data were rearranged according to the row priority method to obtain a two-dimensional matrix marked with thickness values. Finally, the dimensional numerical matrix was converted into a three-dimensional structure image by image processing. The advantage of this method is that it ensures the accuracy of the thickness prediction model and has high reconstruction efficiency.

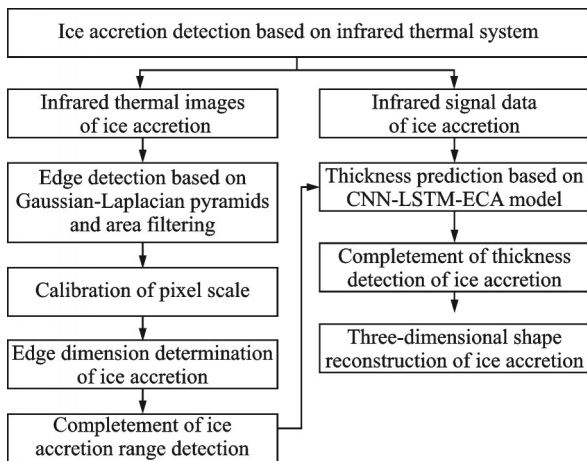


Fig.9 Three-dimensional reconstruction of ice accretion

#### 4.2 Results and discussion of reconstruction

Take the thickness of the ice sample (Fig.2 (b)) calculated in Section 3 is taken as an example for three-dimensional reconstruction. Since the background takes up a lot of data that does not need to be calculated for thickness, it is determined that the calculated ratio of pixel to size (mm) is 1: 2.5 by

scaling the images to remove the background. Thus, the calculation speed has been greatly improved. The reconstruction model is shown in Fig.10. The accuracy of the ice range depends on the pixel scale of the infrared thermal camera, while the accuracy of the thickness depends on the CNN-LSTM-ECA model.

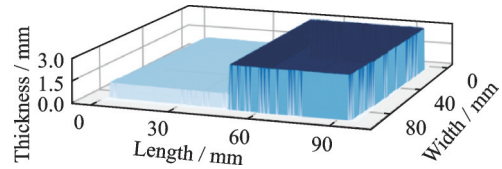


Fig.10 Three-dimensional shape of ice accretion

In the previous research, Li et al.<sup>[32]</sup> used the inverse heat transfer problem for three-dimensional identification of regular ice accretion. However, the main problem is that the infrared thermogram and temperature calibration of ice were carried out under certain experimental conditions. Therefore, a stable ambient temperature should be guaranteed for each test to reduce the measurement deviation. However, the method proposed in this paper goes beyond the limitations of the previous research. The digital signals and pixels collected by the infrared thermal camera are directly used to predict the quantitative value, which reduces the sensitivity of the temperature collected by the camera to the accuracy of the heat transfer model. It also reduces the dimension calculation error caused by temperature values solving in the geometric inverse heat transfer problem. Moreover, it benefits the three-dimensional reconstruction of irregular ice accretion samples.

## 5 Conclusions

An ice detection method was proposed and preliminarily investigated using non-contact flash pulse infrared thermal detection technology based on experimental static ice accretion samples. The feasibility, advantages and disadvantages of the detection method were discussed from three aspects as ice edge detection, ice thickness prediction, and ice shape reconstruction. The following conclusions are drawn:

(1) Although traditional edge detection operators are capable of identifying the outer contour of

some ice samples, it is difficult to accurately detect the step-type boundary on the surface of the ice sample. By contrast, the edge detection algorithm proposed in this paper combines Gaussian-Laplacian pyramid with area filtering to effectively improve the outcome of identifying the internal step-type boundary on the ice surface. However, the drawback is that the noise also increases with the enhancement of features.

(2) An infrared detection ice thickness prediction model (CNN-LSTM-ECA) is proposed that combines CNN and Bi-LSTM with attention mechanism. The model is applicable to extract data time and space feature information and suitable for processing the signal output of infrared detected ice thickness, which improves the accuracy of prediction results. Meanwhile, the CNN-LSTM neural network is used to train and test the dataset. According to the experimental results, the CNN-LSTM-ECA model performs best in ice thickness prediction, and the ECA mechanism can focus attention on important features, thus improving the accuracy of prediction. The CNN-LSTM-ECA model is effective in reducing the noise interference caused by external factors during the infrared detection of ice thickness, showing a certain level of stability and robustness to noise.

(3) The combination of ice accretion range and thickness prediction to reconstruct a three-dimensional model of ice accretion is based on the digital signal and infrared thermal images collected by the flash pulse infrared thermography system. This method can break through the constraint of solving geometric infrared heat transfer inverse problems based on temperature values, and has a wider application prospect.

## Reference

- [1] WANG Y, HAN L, ZHU C, et al. Design of an experimental set-up concerning interfacial stress to promote measurement accuracy of adhesive shear strength between ice and substrate[J]. Transactions of Nanjing University of Aeronautics and Astronautics, 2022, 39(5): 561-568.
- [2] HAN Y, PALACIOS J L, SMITH E C. An experimental correlation between rotor test and wind tunnel ice shapes on NACA 0012 airfoils[C]//Proceedings of SAE 2011 International Conference on Aircraft and Engine Icing and Ground Deicing. Chicago, USA: SAE, 2011.
- [3] BLASCO P M. An experimental and computational approach to iced wind turbine aerodynamics[D]. Pennsylvania: The Pennsylvania State University, 2015.
- [4] STRUCK P, LYNCH C. Ice growth measurements from image data to support ice-crystal and mixed-phase accretion testing[C]//Proceedings of the 4th AIAA Atmospheric and Space Environments Conference. New Orleans, Louisiana: AIAA, 2012.
- [5] IKIDAES A A, SPASOPOULOS D, AMOIROPoulos K, et al. Detection and rate of growth of ice on aerodynamic surfaces using its optical characteristics[J]. Aircraft Engineering and Aerospace Technology, 2013, 85(6): 443-452.
- [6] GONG X, BANSMER S. Laser scanning applied for ice shape measurements[J]. Cold Regions Science and Technology, 2015(115): 64-76.
- [7] WANG Xiaohui, MA Qinglin, KONG Weiliang, et al. Research on aircraft icing detection of super-cooled large droplets for airworthiness certification[J]. Journal of Nanjing University of Aeronautics & Astronautics, 2023, 55(2): 265-273. (in Chinese)
- [8] CARLORS QUITERIO G M, FAUSTO PEDRO G M, JUAN MANUEL S T. Ice detection using thermal infrared radiometry on wind turbine blades[J]. Measurement, 2016 (93): 157-163.
- [9] RIEHM M, GUSTAVSSON T, BOGREN J, et al. Ice formation detection on road surfaces using infrared thermometry[J]. Cold Regions Science and Technology, 2012(83): 71-76.
- [10] RASHID T, KHAWAJA H A, EDVARDBSEN K. Measuring thickness of marine ice using IR thermography[J]. Cold Regions Science and Technology, 2019 (158): 221-229.
- [11] GRZYCH M L, MASON J G, PATNOE M. Ice crystal icing engine event probability estimation apparatus, system, and method: US 9429680B2[P]. 2016-02-10.
- [12] GAO J S, HAN R Y, YU Z J, et al. Near infrared multispectral solution to ice detection on CF composite material wing[J]. Optics and Precision Engineering, 2011, 19(6): 1250-1255.
- [13] WANG X, HU J, WU B, et al. Study on edge extraction methods for image-based icing on-line monitoring on overhead transmission lines[C]//Proceedings of the 2008 International Conference on High Voltage Engineering and Application. [S.l.]: IEEE, 2009.
- [14] LU J, ZHANG H, FANG Z, et al. Application of

- adaptive segmentation threshold in ice thickness recognition[J]. *High Voltage Technology*, 2009, 35(3): 563-567.
- [15] CHI H, TIAN Y. Analysis and research on image edge detection algorithm[J]. *Reliability and Environmental Test of Electronic Products*, 2021, 39(4): 92-97.
- [16] XU Z, JI X, WANG M, et al. Edge detection algorithm of medical image based on Canny operator[J]. *Journal of Physics: Conference Series*, 2021, 1955(1): 012080.
- [17] LI Y, LI C, QU H, et al. Infrared image segmentation method based on improved artificial bee colony sine cosine optimization[J]. *Laser and Infrared*, 2021, 51(8): 1076-1080.
- [18] KONG S, HUANG Z, YANG J. Research status and progress of infrared thermal image nondestructive testing image processing[J]. *Infrared Technology*, 2019, 41(12): 1133-1140.
- [19] LIU X, XU Y, QI H, et al. Hierarchical stripping volume painting based on Gauss Laplace[J]. *Computer Engineering and Science*, 2014, 36(6): 1148-1153.
- [20] ZHU W, LIU J, ZHU M, et al. Improved DR image enhancement algorithm based on Gauss Laplace pyramid[J]. *Chinese Journal of Medical Devices*, 2019, 43(1): 10-13.
- [21] LI Y, XIAO J, ZHU L, et al. Applications of the infrared thermal wave technology in thermal barrier coating thickness testing[J]. *Infrared Technology*, 2017, 39(7): 669-674.
- [22] HUANG X B, LI H B, ZHU Y C. Short-term ice accretion forecasting model for transmission lines with modified time-series analysis by fireworks algorithm[J]. *IET Generation, Transmission and Distribution*, 2018, 12: 1074-1080.
- [23] ZHANG Y, XU X, WANG Z Q. A review of support vector machines and time series forecasting[J]. *Computer Applications and Software*, 2010, 27(12): 127-129, 157.
- [24] ZHANG M, HE J. A review of time series forecasting model research[J]. *Mathematics in Practice and Understanding*, 2011, 41(18): 189-195.
- [25] SHI X, CHEN Z, WANG H, et al. Convolutional LSTM network: A machine learning approach for precipitation nowcasting[C]//*Proceedings of the 28th International Conference on Neural Information Processing Systems — Volume 1*. Montreal, Canada: MIT Press, 2015: 802-810.
- [26] ARGAWAL T, CHOUDHARY P. ALCNN: Attention based lightweight convolutional neural network for pneumothorax detection in chest X-rays[J]. *Biomedical Signal Processing and Control*, 2023, 79(P1): 104126.
- [27] ZHUANG W, CAO Y. Short-term traffic flow prediction based on CNN-BILSTM with multicomponent information[J]. *Applied Sciences*, 2022, 12(17): 8714.
- [28] LI J, LIU H, GUO W, et al. Spatio-temporal prediction model of population activity flow based on deep learning[J]. *Journal of Geomatics*, 2021, 50(4): 522-531.
- [29] CHEN C, QI F. Review of the development of convolutional neural networks and their applications in the field of computer vision[J]. *Journal of Computer Science*, 2019, 46(3): 63-73.
- [30] YUNIARTI A, ARIFIN A Z, SUCIATI N. A 3D template-based point generation network for 3D reconstruction from single images[J]. *Applied Soft Computing*, 2021(111): 107749.
- [31] LOMBARDI M, SAVARDI M, SIGNORONI A. DenseMatch: A dataset for real-time 3D reconstruction[J]. *Data in Brief*, 2021(39): 107476.
- [32] LI Q, HAO L, PAN W, et al. Three-dimensional ice shape detection based on flash pulse infrared thermal wave testing[J]. *Case Studies in Thermal Engineering*, 2022(36): 102196.

**Acknowledgements** This work was supported by the Open Fund of Key Laboratory of Icing and Anti/De-icing (No. IADL20200201) and the National Natural Science Foundation of China (No.62171271).

**Author** Dr. LI Qingying received the Ph.D. degree in Nanjing University of Aeronautics and Astronautics in 2012. Her research is focused on infrared thermal wave detection, aircraft anti/de-icing technology and relevant fields.

**Author contributions** Dr. LI Qingying designed the study, conducted the analysis, interpreted the results and wrote the manuscript. Ms. GOU Yi compiled the models, contributed to data and processed images for the ice detection. Dr. LIU Senyun guided the experimentation, demonstrated the ice detection methods, and revised the manuscript. Prof. YAO Rao contributed to the discussion and background of the study and funding acquisition. All authors commented on the manuscript draft and approved the submission.

**Competing interests** The authors declare no competing interests.

## 基于闪光红外热像技术的积冰探测方法

李清英<sup>1</sup>, 勾一<sup>1</sup>, 刘森云<sup>2</sup>, 么 娆<sup>1</sup>

(1. 上海工程技术大学航空运输学院, 上海 201620, 中国; 2. 中国空气动力研究与发展中心结冰与防除冰重点实验室, 绵阳 621000, 中国)

**摘要:** 结冰探测在防除冰系统运行中起着至关重要的作用。本文提出了利用红外热波检测技术进行了积冰探测, 并运用相关分析技术探讨了积冰边缘、厚度识别与冰形重建的方法。搭建了闪光脉冲红外主动式红外积冰探测实验平台, 制备了规则型与阶跃型积冰样件, 借助红外热像仪采集了受脉冲红外热激励后的积冰红外热信号。运用传统边缘检测方法与新构建的高斯-拉普拉斯金字塔和面积滤波相结合的边缘检测算法进行了积冰边缘识别效果的对比与分析。利用积冰热信号的时空相关性, 提出了在长短时记忆(Long short term memory, LSTM)模型中引入注意力机制建立端到端的红外探测积冰厚度预测模型(Convolutional neural network-long short term memory-efficient channel attention, CNN-LSTM-ECA), 用以预测积冰厚度。此外, 通过结合边缘检测和厚度预测, 进行了阶梯状积冰样件的三维重建。结果表明, 基于高斯-拉普拉斯金字塔和区域滤波的传统边缘检测算法和新的边缘检测算法都可以用于检测冰的外边缘, 但新算法在检测具有内部阶梯边界的冰边缘方面显示出显著的优势。基于信号特征的CNN-LSTM-ECA厚度预测模型在预测精度、稳定性和抗噪声性方面表现良好。重建三维积冰形状的数据来源于采集的数字信号和热图像, 不受温度读数和传热条件的限制, 具有更广阔的应用前景。此项研究为探索一种利用闪光脉冲红外技术进行积冰冰形有效、准确、定量识别提供可参考的方案。

**关键词:** 积冰; 红外探测; 边缘检测; 厚度预测; 三维重建